

# A Novel Passive Mechanism for Flying Robots to Perch onto Surfaces

HaoTse Hsiao<sup>1</sup>, Feiyu Wu<sup>1</sup>, Jiefeng Sun<sup>1</sup>, and Jianguo Zhao<sup>1</sup>

**Abstract**—Perching onto objects can allow flying robots to stay at a desired height at low or no cost of energy. This paper presents a novel passive mechanism for aerial perching onto smooth surfaces. This mechanism is made from a bistable mechanism and a soft suction cup. Different from existing designs, it can be easily attached and detached onto a surface, but it can also hold a large weight when attached to a surface. Further, the mechanism can still work when the suction cup is not precisely aligned with the surface, alleviating the requirement for precise motion control of flying robots. The attachment and detachment are facilitated by the bistable mechanism, while the strong holding is enabled by a locking mechanism that can disable the bistable mechanism. We conduct experiments to characterize the required forces for successful attachment and detachment. We also equip the perching mechanism onto a quadcopter to demonstrate it can be successfully used for perching onto smooth surfaces (e.g., glass). With proper planning and control, the proposed mechanism can be potentially attached to existing quadcopters to perch onto smooth ceilings, vertical walls, or moving vehicles.

## I. INTRODUCTION

Flying robots have been recently widely used for various applications, such as 3D mapping, environmental monitoring, disaster relief, precision agriculture, etc [1]. But most of existing flying robots, especially quadcopters, cannot stay airborne for a long time because of their limited power supply. In this case, it's better that they can perch/land on objects to save energy while maintaining a desired height for specific applications (e.g., long-duration monitoring tasks) [2]. Among all the objects that a flying robot can land onto, smooth surfaces represent an important category. Being able to perch onto smooth surfaces will greatly enhance flying robots' capability. For instance, they can perch onto the windows of high-rise buildings to perform inspections after a storm. They can also safely land onto a ship deck at sea that may be subject to unpredictable waves [3]. They can also be used to land on a moving vehicle that may move on an uneven terrain [4].

Nevertheless, the landing/perching process is nontrivial as it involves a complicated perception, planning, and control process. In order to successfully perch onto a surface, the robot needs to rely on sensors (e.g., camera) to detect the surface, estimate the surface's orientation, plan a trajectory, and then follow the trajectory [5], [6]. It also requires a mechanical mechanism that can attach the robot to the surface. Recently, however, it has been suggested that a properly designed mechanism can be leveraged to enable

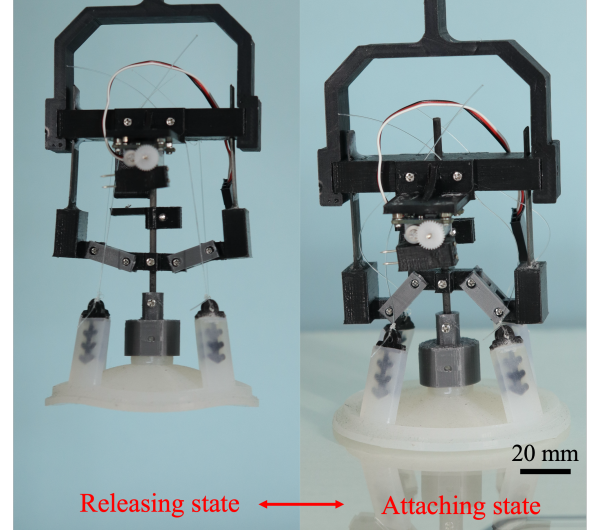


Fig. 1: The prototype of the passive mechanism with its two stable states.

physical intelligence [7] that can alleviate the requirement for planning and control [8], [9].

In recent years, researchers have developed various mechanisms for perching onto surfaces based on dry adhesives, electrostatic forces, suction cups, and other methods. For dry adhesives, a flying robot is equipped with several pads with dry adhesives attached. When the robot contacts a surface, the dry adhesive can ensure the robot to perch onto the surface [6], [10], [11]. For electrostatic forces, a flying robot has pads that can generate electrostatic forces between the pad and the surface when a high voltage is applied [12], [13]. For suction cups, normally miniature vacuum pumps are used to generate a strong attachment between the robot and the surface [14]–[16], but there also exist passive ones that rely on the impact force [17]. Besides the three main methods, there are other methods such as reverse thrust [18], flip and flap [19], etc.

In this paper, we present the design, development, and experimentation of a passive perching mechanism that can be used for flying robots to perch onto smooth surfaces. The mechanism is based on a bistable mechanism and a customized suction cup (Fig. 1). Initially, the suction cup is pulled from the edges by the bistable mechanism through cables, enabling easy attachment onto a surface upon contact. After attachment, we can lock the bistable mechanism to generate a strong attachment force that can hold the flying robot. To detach from the surface, we unlock the bistable

\*This work is partially supported by National Science Foundation under grants IIS-1815476.

<sup>1</sup>All authors are with the Department of Mechanical Engineering at Colorado State University, Fort Collins, CO, 80523, USA

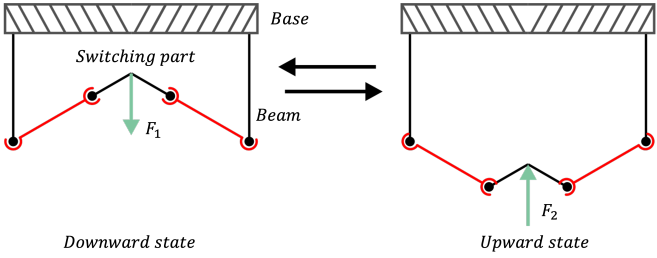


Fig. 2: Diagram of bistable mechanism with two stable states. Left: the top state shows the switching part is at the top. Right: the bottom state shows the switching part is at the bottom. The bistable mechanism can transit between these two states. While applying a downward force  $F_1$ , the top state will transit to the bottom state. On the contrary, While applying an upward force  $F_2$ , the bottom state will transit back to the top state.

mechanism, after which a small force can switch the state of the bistable mechanism to pull the edges of the suction cup to easily detach from the surface.

Our passive perching mechanism has the following advantages compared with existing suction cup-based perching mechanisms. First, it is passive without using vacuum pumps, a heavy part that will decrease the payload capability of a flying robot. Attaching to a surface is realized by using the impact force between the mechanism and the surface while detaching from the surface is realized by the thrust force of the flying robot. Second, it can hold a large weight with the locking mechanism, making it suitable for heavy flying robots. Our experimental results show that with a mass of 40 g for the passive mechanism, it can hold a quadcopter with a total weight of 601 g. Third, the mechanism can still work when the cup is not fully aligned with the surface, alleviating the requirement for precisely controlling the perching orientation.

The rest of this paper is organized as follows. In section II, we explain the working principle of the proposed perching mechanism. In section III, we discuss the design and fabrication of the mechanism. In section IV, we present the experimental results. In section V, we conclude the paper and discuss future works.

## II. WORKING PRINCIPLE

In this section, we introduce the working principle of our mechanism for surface perching. The mechanism includes three main parts: a custom-made soft suction cup, a bistable mechanism, and a locking mechanism.

The soft suction cup can attach onto a flat and smooth surface such as the surfaces of glass, metal, or ground materials. After it attaches to a surface, it can withstand a large pulling force applied at the center to remain in the attached state. However, we can easily detach the cup by pulling the edges of the cup. To facilitate the attachment and detachment of the suction cup from a surface, we integrate the suction cup with a bistable mechanism with two stable states. To maintain the attached state, we use a locking

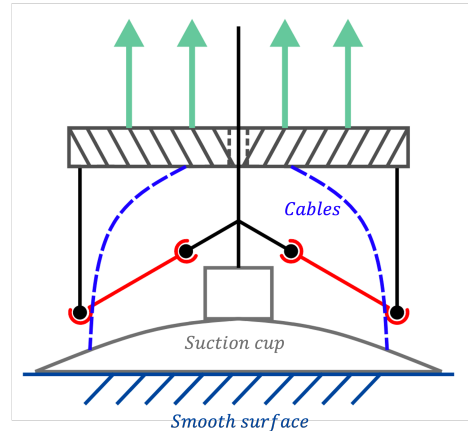


Fig. 3: Diagram of the bistable mechanism integrated with a suction cup.

mechanism. In the following, we first introduce the bistable mechanism, then the integration of the bistable mechanism with the suction cup, and finally the whole mechanism.

### A. Bistable Mechanism

Our passive perching mechanism utilizes a bistable mechanism to achieve two stable states which is shown in Fig. 2. While the downward force  $F_1$  applies on switching part at the top state of the bistable mechanism (left in Fig. 2), the beams are bent out, and the mechanism transits to the bottom state (right in Fig. 2). On the other hand, when an upward force  $F_2$  is applied on the switching part at the bottom state of the bistable mechanism, it changes back to the top state. The detailed working principle for this can be found in our previous work [9].

### B. Bistable Mechanism with a Suction Cup

The bistable mechanism can be integrated with a customized suction cup to facilitate the attachment and detachment from a surface. As shown in Fig. 3, we attach the top part of the suction cup to the switching part of the bistable mechanism. We also use cables to connect the edges of the suction cup to the base of the bistable mechanism.

By properly adjusting the length of the cables, we can ensure that the edges of the cup will bend upward when the bistable mechanism is at the bottom stable state (bottom left of Fig. 4). Such bending will facilitate attachment to the surface since the center part of the cup will contact the surface first and then the edges, ensuring a strong attachment. It will also reduce the requirement for precise alignment between the cup and the surface. The cables can also facilitate the detachment. If we pull the base upward, the cables will drag the edges to let the cup easily detach from the surface.

### C. Working Principle of the Whole Mechanism

With the bistable mechanism integrated with a suction cup, we further add a locking mechanism to ensure the suction cup can remain the attachment when needed. With

the whole mechanism, we explain four main states during a cycle of motion with a simplified sketch (Fig. 4). To illustrate, consider the case that the mechanism is installed on the bottom of the quadcopter with an initial releasing state  $S_r$ . Note that the mechanism can also be placed on the top or side to perch onto the bottom of a horizontal surface or a vertical surface. During a cycle of motion, the mechanism can undergo the following states: an initial releasing state  $S_r$ , an attached state  $S_a$ , a locking state  $S_l$ , and an intermediate state  $S_i$ . In the following, we discuss the transitions between these states.

**Process  $P_{ra}$  (from  $S_r$  to  $S_a$ ):** When the mechanism is at the initial state  $S_r$ , the suction cup cannot form a close enclosure to suck on the surface because its edges are pulled by cables from the base. When the quadcopter lands on a surface, the suction cup will contact the surface and the downward force from weight of the quadcopter will generate an impact force to push the bistable mechanism transit to the opposite state. Meanwhile, the cables will loosen to allow the edges of the cup to contact the surface. In this case, the suction cup can create the suction force to attach onto the surface, and the mechanism is at the attachment state  $S_a$ .

**Process  $P_{al}$  (between  $S_a$  and  $S_l$ ):** When the quadcopter attaches to the surface, we can use a locking mechanism to ensure it remains attached (state  $S_l$ ), and we can also unlock the mechanism to make it return to state  $S_a$ . To do this, we attach a rod to the bistable mechanism at the center that passes through a hole at the base. To lock the whole mechanism, we can disable the bistable mechanism by blocking the relative displacement between the base and center rod. In this case, the cables will remain loose and cannot apply force to the edge of the suction cup. Instead, all the force is applied at the top center of the suction cup, allowing the suction cup to stay in place even with a very large upward force. To unlock the mechanism, we can enable the bistable mechanism to allow relative displacement between the base and center rod. In this case, the system can return back to state  $S_a$ .

**Process  $P_{ai}$  (from  $S_a$  to  $S_i$ ):** At state  $S_a$ , when the quadcopter flies upward, generating an upward force that will transit the whole mechanism to an intermediate state  $S_i$ . During this process, the suction cup is still attached onto the surface because all upward force is applied to the center of the suction cup. Meanwhile, the cables are gradually tensioned but it is still not fully tensioned to pull the edge of the suction cup.

**Process  $P_{ir}$  (from  $S_i$  to  $S_r$ ):** After the mechanism crosses state  $S_i$ , the state will rapidly transit to the initial state  $S_r$ . During this process, the cables start to pull the edge of the suction cup with tension and the air leaks into the suction cup to release the cup from the surface. Then, the quadcopter can fly away from the surface.

The whole process can form a loop to allow the passive mechanism to successfully accomplish perching/landing onto a surface. Because the edges are pulled by the cables at the initial state  $S_i$ , the mechanism can still work when the cup is not fully aligned with the surface. In other words, we will

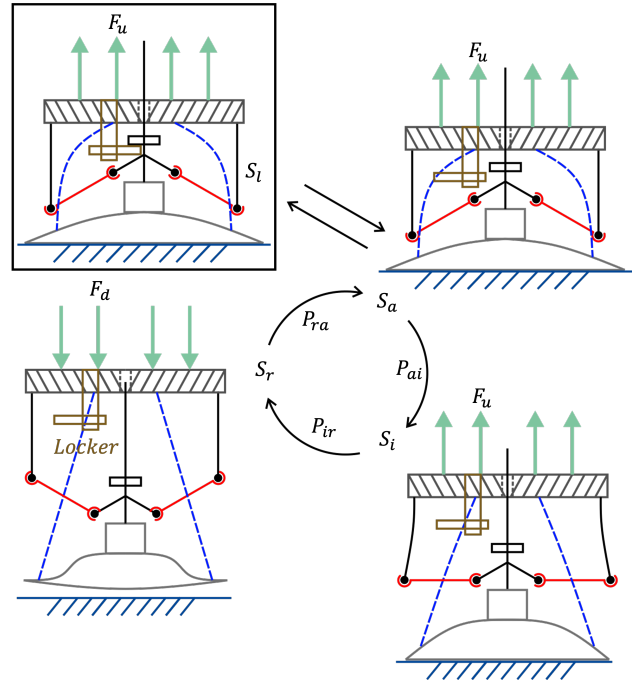


Fig. 4: The diagram of the perching mechanism's working principle. The bottom left sketch shows the initial releasing state  $S_r$ . While applying the downward  $F_d$ ,  $S_r$  will transit to attaching state  $S_a$  (top right sketch). If the locker (brown color sketch) locks, the mechanism will transit to locking state  $S_l$  (top left sketch), and it can also go back to  $S_a$  when unlocked. When at state  $S_a$ , the upward force will make it first transit to the intermediate state  $S_i$  (bottom right), which will rapidly switch back to the original state  $S_r$ .

not need to control the perching orientation very precisely.

### III. DESIGN AND FABRICATION

In this section, we elaborate the design and fabrication of the three main parts: bistable mechanism, suction cup, and locker, which are individually shown in Fig. 5a-c. A whole assembly of all the three mechanisms without the cables is shown in Figure 5d.

The bistable mechanism shown in Fig. 5a includes one switch part, two links for connection between the switch part and beam heads, two beam heads for connection between the beams and links, one rigid base with a hole for linear guide rod, and linear guide rod to guarantee vertical displacement, which are all 3D printed parts. Furthermore, the two bendable beams are flat carbon fiber (Width  $\times$  Thickness: 7.9  $\times$  0.8 mm, CF312032048, Goodwinds Composites LLC). We can also adjust the effective length of the carbon fiber using screws.

The suction cup is connected to the bistable mechanism's linear guide rod through a 3D printed cup head. Four 3D printed pullers are embedded in the suction cup's parts where the cables are connected to enhance the strength as shown in Fig. 5b. Detailed fabrication of the suction cup will be introduced later.

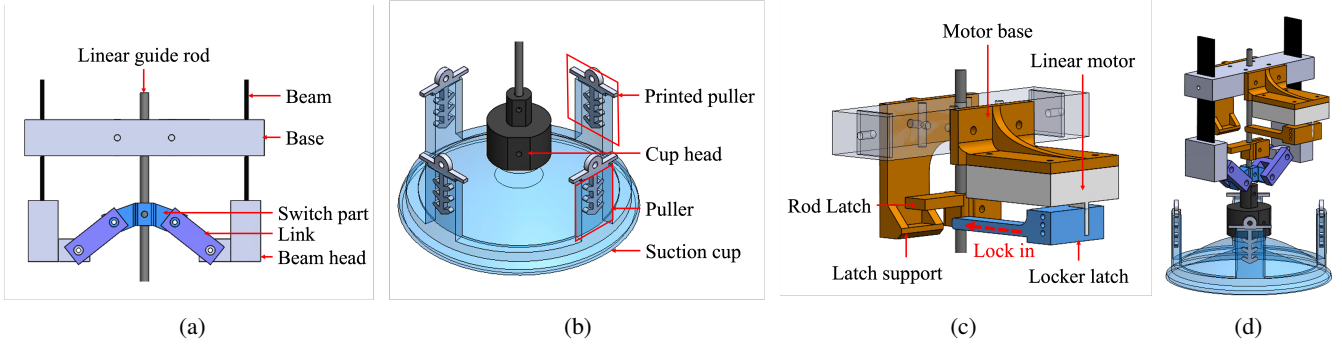


Fig. 5: The structure diagrams of (a) the bistable mechanism part, (b) the suction cup part (c) the locker part, and (d) the assembly of the parts.

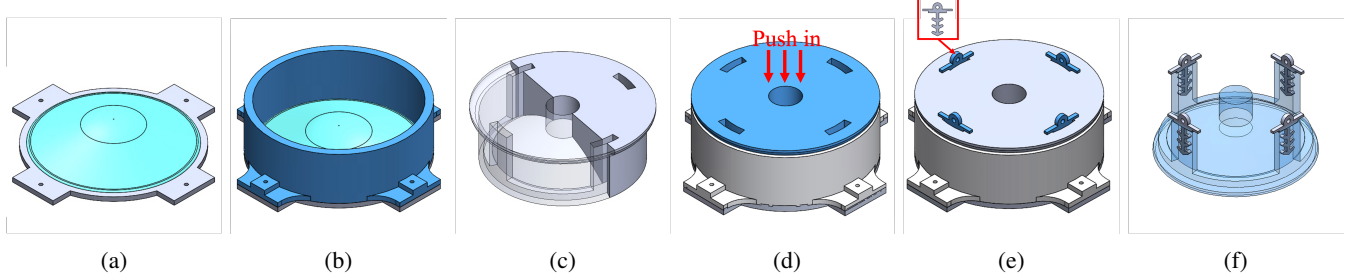


Fig. 6: (a) Coating a thin layer of XTC-3D (light blue color) on the bottom mold to fabricate a smooth surface. (b) combining the wall mold with bottom mold, then the dragon skin is filled into the mold until half level. (c) The cross-section view of top mold. (d) The top mold is slowly plugged into the combined mold. (e) The pullers (top left sketch) is placed in the four holes and pouring the additional materials to fill into the mold fully, then to put the mold into the vacuum for removing the bubbles inside the dragon skin 30 materials. (f) The suction cup can be demolded after four hours curing.

The locker part can lock the bistable mechanism to block the relative displacement between the base and linear guide rod. Figure 5c shows the locker part that includes the rod latch, the motor base, the latch support, and the locker latch. The motor base mounts the linear servo motor (GS1502) on the base of the bistable mechanism. The red dash arrow shows the direction of the locker latch will move in. While it is locked, the relative displacement between the base and linear guide rod is restricted, and the state of the mechanism cannot switch from attaching state to next state.

The suction cup part is fabricated using silicone rubber (Dragon Skin 30, Smooth-On Inc.) with an assembly of three 3D printed molds: the bottom mold, the surrounding wall mold, and the top mold as shown in Fig. 6. The fabrication procedure is shown in Fig. 6. First, the upper surface of the bottom mold is painted with a layer of XTC-3D (Smooth-On Inc.) to form a smooth surface (Fig. 6a) that will ensure a good vacuum seal of the suction cup. Then, the surrounding wall mold is screwed on the bottom mold and the dragon skin 30 is filled into it (Fig. 6b).

The top mold can be placed inside of the surrounding wall mold and a cross-section view is shown in 6c. After filling some dragon skin 30 to the half level of volume of the combined mold, the top mold is assembled, during the process, we slowly push the top mold to avoid introducing more air or bubbles (Fig. 6d). Then, the whole mold with

filled dragon skin 30 is put into a vacuum for removing the air bubbles. Finally, the printed pullers which include some fin features are plugged into the hole of the top mold to increase the strength of the pulling parts (Fig. 6e). Then, we need to cure the part for four hours before demolding (Fig. 6f).

#### IV. EXPERIMENTS AND RESULTS

In this section, we experimentally characterize the passive mechanism and conduct a perching/landing experiment. For the passive mechanism, we mainly obtain the force-displacement relationship for different parts to verify the design of the passive mechanism in Sec. II-C and Fig. 4. Note that all force experiments are measured by using a motorized test stand (ESM303, Mark-10). For showing every force-displacement relationship experiment, we use the means and shade errors to represent 3 tests.

##### A. Maintenance Force of $S_r$

As the passive mechanism is at  $S_r$ , we need to ensure the bistable mechanism stays at the bottom stable states. This means the tension force in the string  $F_s$  should not be able to switch the state. In other words,  $F_s$  should be smaller than the maximum of bistable switching force  $F_b$  to stay in the state  $S_r$ . Therefore, we set up the experiments to test  $F_s$  and  $F_b$ .

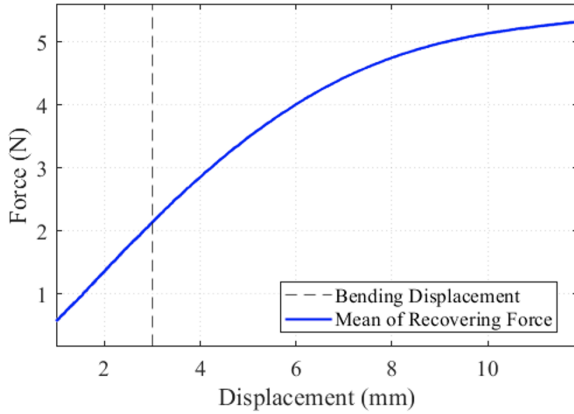


Fig. 7: The force-vertical-displacement relationship of the suction cup while the strings pulls the edge of the suction cup from 0 to 10 mm. The dark dash line is using 2.1 N to bend suction cup with displacement 3 mm.

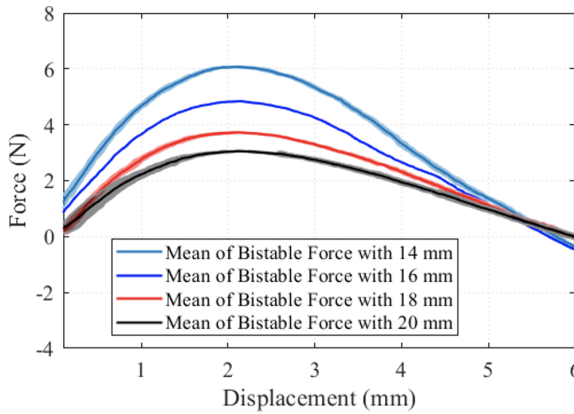


Fig. 8: The force-displacement relationship of bistable mechanism. It shows  $F_d$  with effective beams from 14 mm to 20 mm. To instance, while the case of vertical displacement of bending suction cup is 3.5 mm with 2.21 N, the effective length of beams is required 18 mm at least to keep  $S_r$ .

First, we experimentally obtain  $F_s$  with respect to vertical displacement by using the test stand to pull the strings fixed to the pulling part of the suction cup and record the force. The result is shown in Fig. 7 where force increases with the vertical displacement from 0 to 10 mm. However, the vertical displacement of the suction cup's edge during is about 3 mm for our experiments. Therefore, the maximum of  $F_s$  is about 2.1 N when the displacement is 3 mm (black dash line in Fig. 7). Note that the maximum string force is adjustable by changing the length of strings.

Second, the bistable switching force  $F_b$  is related to the bending stiffness of the beam that combines a flat carbon fiber rod and a 3D printed beam head. We directly measured the relationship between the effective length of beams and  $F_b$ . The  $F_b$  changing with respect to the displacement of the linear guide rod is shown in Fig. 8. To keep  $S_r$ , the effective length of beams should be adjusted to make sure

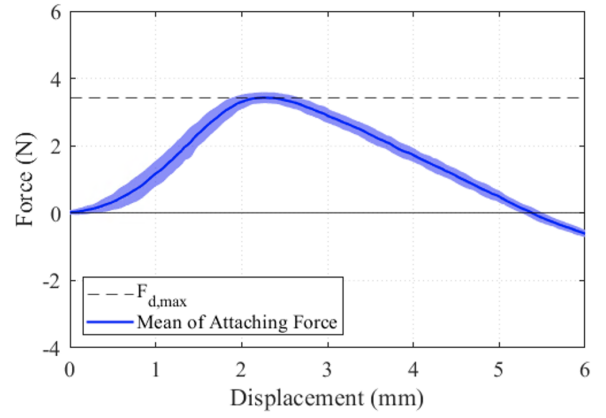


Fig. 9: The force-displacement relationship of the passive mechanism with  $F_d$ . The black dash line is  $F_{d,max}$  to transit the state from  $S_r$  to  $S_a$ .

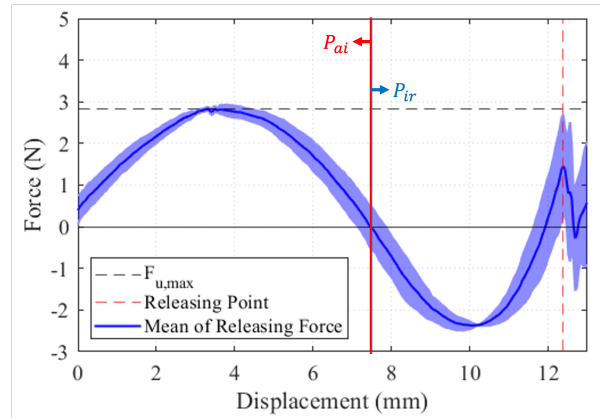


Fig. 10: The force-displacement relationship of the passive mechanism with  $F_u$ . It shows  $P_{ai}$  which is before the red-blue line and  $P_{ir}$  which is after the red-blue line. The black dash line is  $F_{d,max}$  to transit the state from  $S_r$  to  $S_a$ . The red dash line is the releasing point to achieve  $S_r$ .

the maximum value of  $F_b$ :  $F_{b,max} > F_s$ . For example, if the maximum of  $F_s$  is about 2.1 N (corresponding to 3 mm), the effective length of the beams is required to be less than 20 mm in Fig. 8.

### B. Attaching Force Experiment

The attaching force is the maximum value of the measured downward force  $F_{d,max}$  to let  $S_r$  transit to  $S_a$ . The force-displacement relationship of  $P_{ra}$  is shown in Fig. 9. While  $F_d$  is applied on the base, once the  $F_d$  conquers  $F_{d,max}$  which is 3.43 N with the effective length of beams 20 mm, the suction cup at  $S_r$  will transit to  $S_a$ . The weight of the quadcopter in our lab is 5.89 N (601 g) with the passive mechanism, which is greater than  $F_{d,max} = 3.43$  N with the effective length of beams 20 mm. Therefore, the quadcopter can do passively attaching and land on smooth and flat surfaces.

At  $S_a$ , the passive mechanism can transit to  $S_l$  by triggering the locker. Once it is at  $S_l$ , the attaching force relies on

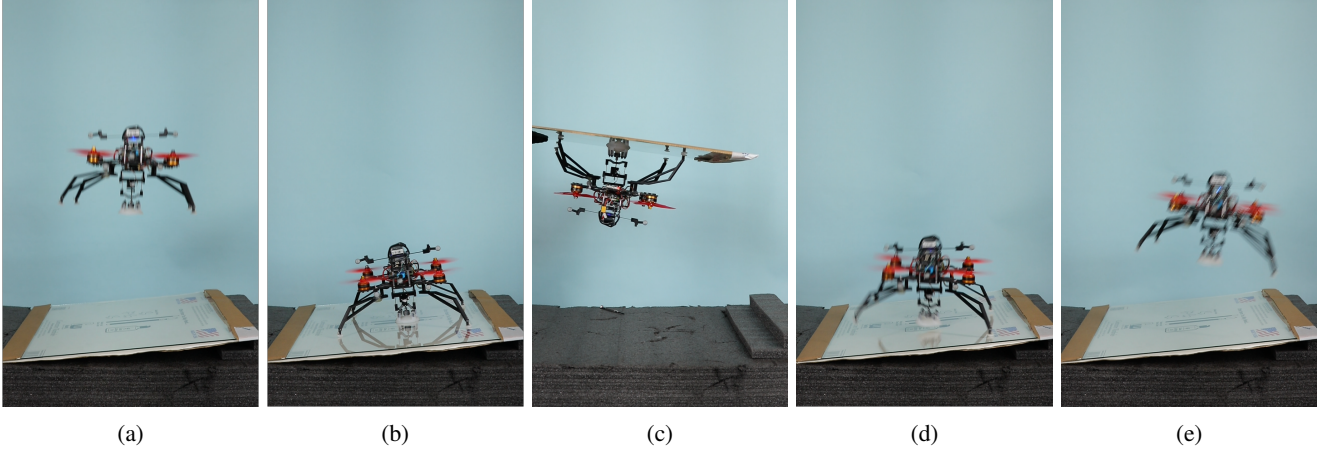


Fig. 11: Perching experiment. (a) The passive mechanism can keep  $S_r$  during the flight. (b) The quadcopter with the passive mechanism can land on a glass plate with 6 degrees tilting angle. (c) Once the locker is locked in, the passive mechanism cannot transit to  $S_i$  and the quadcopter keeps attaching on the glass. even though the glass is flipped upside down. (d) While the mechanism is unlocked, the quadcopter can fly up and the passive mechanism transit to  $S_r$ . (e) Then, the quadcopter can fly away.

the force of the suction cup and the force is stronger than 10 N. However, the test range of our force gauge is less than 10 N. Therefore, we will not show the force-displacement relationship to verify it.

### C. Releasing Force Experiment

A releasing force should be applied to switch the state from  $S_a$  to  $S_i$ , after which the state will be automatically transit to the initial state  $S_r$ . We also experimentally obtain the required releasing force for the developed mechanism. Fig. 10 shows the force-displacement relationship during  $P_{ai}$  and  $P_{ir}$ . In Fig. 10, the boundary solid line separates the whole process into  $P_{ai}$  and  $P_{ir}$ . During  $P_{ai}$  which is before the red-blue solid line, the strings are not pulling the edge of the suction cup. If  $F_u$  crosses the maximum of the upward force  $F_{u,max}$  with 2.83 N with an effective length of the beams 20 mm, the process will cross  $S_i$  and keep going to  $P_{ir}$  which is after the red-blue solid line. During  $P_{ir}$ , the strings start pulling the edge of the suction cup. Therefore, after the vertical displacement is at 12.38 mm (red dash line), the suction cup releases the surface and the state completes the transition to  $S_r$ .

### D. Aerial Perching Experiment

We conduct the aerial perching experiment to verify the working principle of the passive mechanism. The mechanism is fixed onto the bottom of a customized quadcopter developed in our lab. The total weight of the quadcopter is 601 g with the mechanism and the max thrust of the quadcopter is about 907 g. Therefore, the effective length of the beams is set at 20 mm with 2.83 N which is less than the payload of about 3 N (306 g). Fig. 11 shows the aerial perching experiment results. Figure 11a shows the quadcopter carries the passive mechanism in  $S_r$  state while it is hovering. The vertical displacement of the suction cup is 3 mm. Then, the quadcopter lands on the smooth glass with a tilting angle

of 6 degrees, and the passive mechanism transits the states from  $S_r$  to  $S_a$  (Fig. 11b). After that, the locker is locked in and the state transits to  $S_l$ . Consequently, the quadcopter with the locked mechanism can attach onto the glass even though the glass plate is shaking or upside down (Fig. 11c). Finally, when the mechanism is unlocked, the quadcopter at  $S_a$  can fly away and the state will transits to  $S_r$  (Fig. 11d and Fig. 11e).

Since it is difficult to fly the quadcopter up from a surface with a large tilted angle due to the large recovery moment and our confined flying space, we conduct several landing experiments by manually dropping the quadcopter to surfaces with different angles to demonstrate the robustness of the perching mechanism. Additional experiments are shown in the supplementary video.

## V. CONCLUSIONS

In this work, we presented a novel passive mechanism that can be equipped on a flying robot to allow for its perching. The mechanism can attach onto and detach from a smooth surface automatically. The softness of the suction cup allows the mechanism can significantly increase the robustness of the attaching process for surfaces with different tilting angles.

We introduced the working principle of the mechanism and its fabrication process. Experiments are conducted to characterize the mechanism and the design guideline were also discussed. The final demonstration shows that the mechanism installed on the bottom of a quadcopter allows it to perch on surfaces with different tilting angles. When the locking mechanism is locked, the mechanism can reliably stick to the surface. Once unlocked, the mechanism can detach from the surfaces when the quadcopter takes off. We envision that the mechanism will be implemented on a variety of flying robots to allow them attaching onto smooth fixed surfaces such as ceilings, vertical walls, or moving surfaces of vehicles, ships, or even other flying robots.

## REFERENCES

- [1] D. Floreano and R. J. Wood, "Science, technology and the future of small autonomous drones," *Nature*, vol. 521, no. 7553, pp. 460–466, 2015.
- [2] K. Hang, X. Lyu, H. Song, J. A. Stork, A. M. Dollar, D. Kragic, and F. Zhang, "Perching and resting—a paradigm for uav maneuvering with modularized landing gears," *Science Robotics*, vol. 4, no. 28, p. eaau6637, 2019.
- [3] J. L. Sanchez-Lopez, J. Pestana, S. Saripalli, and P. Campoy, "An approach toward visual autonomous ship board landing of a vtol uav," *Journal of Intelligent & Robotic Systems*, vol. 74, no. 1, pp. 113–127, 2014.
- [4] T. Baca, P. Stepan, V. Spurny, D. Hert, R. Penicka, M. Saska, J. Thomas, G. Loianno, and V. Kumar, "Autonomous landing on a moving vehicle with an unmanned aerial vehicle," *Journal of Field Robotics*, vol. 36, no. 5, pp. 874–891, 2019.
- [5] H. Zhang, B. Cheng, and J. Zhao, "Optimal trajectory generation for time-to-contact based aerial robotic perching," *Bioinspiration & biomimetics*, vol. 14, no. 1, p. 016008, 2018.
- [6] J. Thomas, M. Pope, G. Loianno, E. W. Hawkes, M. A. Estrada, H. Jiang, M. R. Cutkosky, and V. Kumar, "Aggressive flight with quadrotors for perching on inclined surfaces," *Journal of Mechanisms and Robotics*, vol. 8, no. 5, 2016.
- [7] M. Sitti, "Physical intelligence as a new paradigm," *Extreme Mechanics Letters*, vol. 46, p. 101340, 2021.
- [8] H. Zhang, J. Sun, and J. Zhao, "Compliant bistable gripper for aerial perching and grasping," in *2019 International Conference on Robotics and Automation (ICRA)*. IEEE, 2019, pp. 1248–1253.
- [9] H. Zhang, E. Lerner, B. Cheng, and J. Zhao, "Compliant bistable grippers enable passive perching for micro aerial vehicles," *IEEE/ASME Transactions on Mechatronics*, 2020.
- [10] L. Daler, A. Klaptocz, A. Briod, M. Sitti, and D. Floreano, "A perching mechanism for flying robots using a fibre-based adhesive," in *2013 IEEE International Conference on Robotics and Automation*. IEEE, 2013, pp. 4433–4438.
- [11] A. Kalantari, K. Mahajan, D. Ruffatto, and M. Spenko, "Autonomous perching and take-off on vertical walls for a quadrotor micro air vehicle," in *2015 IEEE International Conference on Robotics and Automation (ICRA)*. IEEE, 2015, pp. 4669–4674.
- [12] M. Graule, P. Chirarattananon, S. Fuller, N. Jafferis, K. Ma, M. Spenko, R. Kornbluh, and R. Wood, "Perching and takeoff of a robotic insect on overhangs using switchable electrostatic adhesion," *Science*, vol. 352, no. 6288, pp. 978–982, 2016.
- [13] S. Park, D. S. Drew, S. Follmer, and J. Rivas-Davila, "Lightweight high voltage generator for untethered electroadhesive perching of micro air vehicles," *IEEE Robotics and Automation Letters*, vol. 5, no. 3, pp. 4485–4492, 2020.
- [14] H. Tsukagoshi, M. Watanabe, T. Hamada, D. Ashlih, and R. Iizuka, "Aerial manipulator with perching and door-opening capability," in *2015 IEEE International Conference on Robotics and Automation (ICRA)*. IEEE, 2015, pp. 4663–4668.
- [15] C. C. Kessens, J. Thomas, J. P. Desai, and V. Kumar, "Versatile aerial grasping using self-sealing suction," in *2016 IEEE international conference on robotics and automation (ICRA)*. IEEE, 2016, pp. 3249–3254.
- [16] S. Liu, W. Dong, Z. Ma, and X. Sheng, "Adaptive aerial grasping and perching with dual elasticity combined suction cup," *IEEE Robotics and Automation Letters*, vol. 5, no. 3, pp. 4766–4773, 2020.
- [17] H. W. Wopereis, T. Van Der Molen, T. Post, S. Stramigioli, and M. Fumagalli, "Mechanism for perching on smooth surfaces using aerial impacts," in *2016 IEEE international symposium on safety, security, and rescue robotics (SSRR)*. IEEE, 2016, pp. 154–159.
- [18] J. Bass and A. L. Desbiens, "Improving multirotor landing performance on inclined surfaces using reverse thrust," *IEEE Robotics and Automation Letters*, vol. 5, no. 4, pp. 5850–5857, 2020.
- [19] Z. Huang, S. Li, J. Jiang, Y. Wu, L. Yang, and Y. Zhang, "Biomimetic flip-and-flap strategy of flying objects for perching on inclined surfaces," *IEEE Robotics and Automation Letters*, vol. 6, no. 3, pp. 5199–5206, 2021.